CLINICAL EPIGENETICS

RESEARCH Open Access

Hypermethylation of the 5′ CpG island of the $p14^{ARF}$ flanking exon 1β in human colorectal cancer displaying a restricted pattern of p53 overexpression concomitant with increased MDM2 expression

Christine Nyiraneza[1], Christine Sempoux[2], Roger Detry[3], Alex Kartheuser[3] and Karin Dahan[1,4*]

Abstract

Background: It has been suggested that inactivation of $p14^{ARF}$, a tumor suppressor central to regulating p53 protein stability through interaction with the MDM2 oncoprotein, abrogates p53 activity in human tumors retaining the wild-type *TP53* gene. Differences in expression of tumor suppressor genes are frequently associated with cancer. We previously reported on a pattern of restricted p53 immunohistochemical overexpression significantly associated with microsatellite instability (MSI), low *TP53* mutation frequency, and MDM2 overexpression in colorectal cancers (CRCs). In this study, we investigated whether $p14^{ARF}$ alterations could be a mechanism for disabling the p53 pathway in this subgroup of CRCs.

Results: Detailed maps of the alterations in the $p14^{ARF}$ gene were determined in a cohort of 98 CRCs to detect both nucleotide and copy-number changes. Methylation-specific PCR combined with bisulfite sequencing was used to evaluate the prevalence and distribution of $p14^{ARF}$ methylation. $p14^{ARF}$ alterations were then correlated with MSI status, *TP53* mutations, and immunohistochemical expression of p53 and MDM2. The frequency of $p14^{ARF}$ mutations was extremely low (1/98; 1%), whereas coexistence of methylated and unmethylated alleles in both tumors and normal colon mucosa was common (91/98; 93%). Only seven of ninety-eight tumors (7%) had a distinct pattern of methylation compared with normal colon mucosa. Evaluation of the prevalence and distribution of $p14^{ARF}$ promoter methylation in a region containing 27 CpG sites in 35 patients showed a range of methylated CpG sites in tumors (0 to 25 (95% CI 1 to 13) versus 0 to 17 (95% CI 0 to 2)) in adjacent colon mucosa ($P = 0.004$). Hypermethylation of the $p14^{ARF}$ promoter was significantly correlated with the restricted p53 overexpression pattern ($P = 0.03$), and MDM2 overexpression ($P = 0.02$), independently of MSI phenotype. Although no significant correlation between $p14^{ARF}$ methylation and *TP53* mutational status was seen ($P = 0.23$), methylation involving the proximal CpG sites within the 5′ CpG flanking exon 1β was present more frequently in tumors with restricted p53 overexpression than in those with diffuse p53 overexpression (range of methylated clones 17 to 36% (95% CI 24 to 36%) versus range 0 to 3% (95% CI 0 to 3%), $P = 0.0003$).

Conclusion: $p14^{ARF}$ epigenetic silencing may represent an important deregulating mechanism of the p53-MDM2-$p14^{ARF}$ pathway in CRCs exhibiting a restricted p53 overexpression pattern.

* Correspondence: karin.dahan@uclouvain.be
[1]Center for Human Genetics, Université Catholique de Louvain, Cliniques universitaires Saint-Luc, Avenue Hippocrate 10, Brussels B-1200, Belgium
[4]Institute of Pathology and Genetics, Avenue Georges Lemaître 25, Gosselies 6041, Belgium
Full list of author information is available at the end of the article

Background

The correct functioning of the p53-MDM2-p14^{ARF} pathway requires a delicate balance between the opposing effects of its different components [1-3]. Genetic and epigenetic alterations have been shown to distort this balance in various human malignancies, allowing tumor cells to over-ride the tumor suppressor activity of the p53 protein, thereby facilitating neoplastic conversion [4]. In the vast majority of human neoplasia, including colorectal cancer (CRC), deregulation of the p53 pathway usually occurs by direct inactivation of the *TP53* gene itself; this occurs mainly via point mutations [5], which usually increase the stability of the mutant p53 protein, leading to its overexpression [6]. However, a significant proportion of CRCs, which include mainly microsatellite instability-high (MSI-H) CRCs, and a subset of microsatellite-stable (MSS) sporadic CRCs, display a particular immunohistochemical p53 expression pattern characterized by an accumulation of p53 protein restricted to a limited number of tumor cells, a profile that we previously termed 'restricted p53 overexpression' [7]. This CRC subgroup has an extremely low frequency of *TP53* mutation, and displays overexpression of MDM2 and normal expression of p21, suggesting that deregulation of p53 pathway in this CRC subgroup may be due to other alternative mechanisms than *TP53* mutation.

Inactivation of the *p14^{ARF}* gene has been proposed as a mechanism that is functionally equivalent to an inactivating *p53* mutation, in that it disrupts p53 activity in tumors retaining the wild-type *TP53* gene [4], and more particularly in sporadic MSI-H CRC [8,9]. In this study, we examined whether *p14*^{ARF} inactivation could be one of the mechanisms disturbing the p53 pathway in CRCs, particularly in tumors displaying a restricted p53 overexpression pattern. Therefore, we conducted detailed genetics and epigenetics analysis of the *p14*^{ARF} gene in CRC tumors for which we had complete data on MSI status and DNA mismatch repair deficiency or sufficiency, and we investigated the relationships between *p14*^{ARF} alterations and MSI phenotype, between *p14*^{ARF} alterations and the p53 protein expression pattern and its mutational status, as well as with MDM2 protein expression.

Results

p14^{ARF} gene alterations in colorectal cancer

In our sample, we found that *p14^{ARF}* mutations were extremely rare; we detected only a previously reported point mutation in one sample (1/98; 1%). This somatic missense mutation was detected in exon 2 and corresponds to a C→T transition on a CpG dinucleotide site, affecting the codon 121 (p.Ala121Val) for the *p14^{ARF}* gene, and the codon 107 (p.Arg107Cys) for the *p16/CDKN2A* gene. Of the ninety-six patients, five (5%) patients, including two of the five patients with Lynch syndrome (hereditary non-polyposis colorectal cancer (HNPCC); OMIM #120435) were carriers of a polymorphic variant corresponding to a substitution of G→A in codon 148 in exon 2 (p.Ala148Thr) affecting only the *p16/CDKN2A* open-reading frame. Gene dosage detected no copy-number changes in any of the 98 CRCs examined.

p14^{ARF} promoter methylation in tumors and adjacent colon mucosa from patients with colorectal cancer

Overall, MSP analysis within the 5′ CpG island of *p14*/ARF flanking exon 1β identified coexistence of methylated and unmethylated alleles in tumors and matched adjacent normal-appearing colon mucosa in 91 of the 98 patients (Figure 1 A). By contrast, a distinct methylation

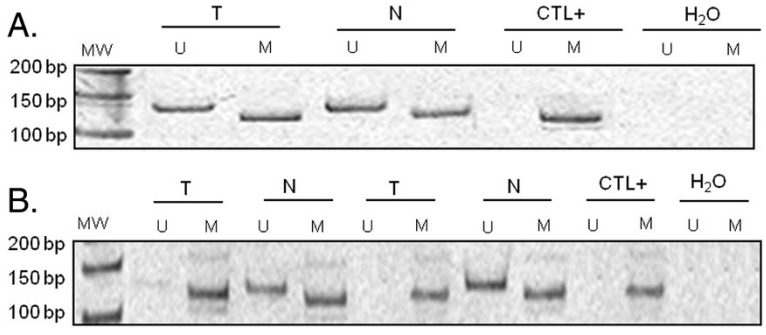

Figure 1 Methylation of the *p14*^{ARF} promoter in tumors and normal colon mucosa from patients with colorectal cancer (A) *p14*^{ARF} promoter methylation analysis by methylation-specific PCR revealed coexistence of both unmethylated (U) and methylated (M) PCR products in tumor (T) and adjacent colon mucosa (N). (**B**) Extensive methylation of *p14*^{ARF} promoter in tumors. The methylated PCR product was predominantly detected in tumor, whereas the adjacent colon mucosa produced both the unmethylated and methylated PCR products. MW, standard molecular weight, control +, positive control for methylated allele, (bisulfite-modified genomic blood DNA pretreated with the CpG methylase (M.SssI)); H_2O, negative control with water only.

profile indicating heavy methylation was seen in seven of the ninety-eight (7.1%) CRCs examined. In these tumors, MSP results identified only methylated alleles in tumors, whereas matched adjacent normal colon mucosa contained both methylated and unmethylated PCR products (Figure 1 B).

Evaluation of density of *p14*^{ARF} promoter methylation in tumors and normal colon mucosa from patients with colorectal cancer

Next, we evaluated the degree of *p14*^{ARF} promoter methylation, limiting the analysis to tumors and corresponding adjacent colon mucosa from 35 randomly selected patients (Table 1), including one of the seven CRCs that was identified as having heavy methylation by MSP (sample T2, Table 1).

Using BGS, we analyzed methylation within the 5′ CpG island of *p14*^{ARF} flanking exon 1β, targeting a region containing 27 individual CpG sites, including all the CpG sites analyzed by MSP in this region (see Additional file 1: Figure S1). BGS showed different *p14*^{ARF} promoter methylation levels among the 35 tumors and adjacent colon mucosa tested, with the highest methylation levels recorded in tumor samples (Figure 2, Figure 3). Of the 35 tumors examined, the range of fully methylated CpG was 0 to 25 and the median was 9 (95% CI 1 to 13), whereas in paired normal colon mucosa the range was 0 to 17 and the median 0 (95% CI 0 to 2) ($P = 0.004$). Of the thirty-five tumors, eighteen (51%) were extensively methylated (>9/27 CpG sites methylated, median of fully methylated CpG sites), six (17%) were partially methylated (>3/27 CpG sites partially methylated, median of partially methylated CpG sites), and 11 (32%) were unmethylated (Table 2).

Although the majority of normal colon mucosa tested (69%) showed a significantly low frequency of methylation compared with matched tumor samples ($P = 0.0019$) (Table 2), extensive methylation was detected in the normal colon mucosa from six patients, including a patient with Lynch syndrome (N7; Figure 3) with a germline mutation in the *MLH1* gene (Table 1) and five patients with sporadic CRC: two MSS tumors (N1, N29; Figure 3) and three MSI-H tumors (N4, N5, N22; Figure 3) with activating V600E *BRAF* somatic mutation associated with *MLH1* epigenetic silencing (Table 1).

Correlation between *p14*^{ARF} promoter methylation, clinicopathological features, p53 pathway alterations, and microsatellite instability status in colorectal cancer

Further, we compared *p14*^{ARF} methylation data from the 35 randomly selected patients analyzed by BGS with their clinicopathological features and the molecular changes in their tumors. No significant association was seen between *p14*^{ARF} methylation and either age or gender (Table 2). Although the majority of right-sided colon tumors (7/10) had increased *p14*^{ARF} methylation, no significant association between *p14*^{ARF} methylation and tumor location was seen (Table 2). Correlation analysis identified a significant association between *p14*^{ARF} hypermethylation and poorly differentiated or mucinous tumors ($P = 0.0270$) (Table 2), but no significant association between *p14*^{ARF} methylation and clinical stage was seen (Table 2). Compared with tumors exhibiting negative and diffuse patterns of p53 protein immunohistochemical expression, the tumors displaying a restricted p53 overexpression profile (15/17) showed a significant increase in *p14*^{ARF} methylation ($P = 0.0274$) (Table 2). *p14*^{ARF} methylation was also significantly associated with MDM2 overexpression ($P = 0.0223$) (Table 2). Most tumors exhibiting *p14*^{ARF} hypermethylation showed an absence of *TP53* mutation (19/24; 79%), but no significant association between *p14*^{ARF} promoter methylation and *TP53* mutational status was seen (Table 2). MSI-H CRCs were more frequently hypermethylated than MSI-low (MSI-L)/MSS CRCs ($P = 0.0539$) (Table 2). However, after stratification by p53 immunohistochemical expression pattern, the relationship between MSI status and *p14*^{ARF} methylation was no longer significant (Figure 4).

Quantification and distribution of *p14*^{ARF} promoter methylation in tumors and normal colon mucosa from patients with colorectal cancer

We evaluated the density and the distribution of methylation within the 5′ CpG island of the *p14*^{ARF} promoter region and exon 1β. Using bisulfite genomic cloning and direct sequencing, we analyzed 200 clones obtained from 10 tumors and matched adjacent colon mucosa. For each clone, the methylation status of each individual CpG site was determined (Figure 5). For all 27 CpG sites evaluated, we found a significantly ($P < 0.0001$) increased number of methylated clones in tumors (median 38%; 95% CI 25 to 41%; range 13 to 47%) compared with the adjacent normal colon mucosa (median 9%; 95% CI 5 to 13%; range 1 to 24%) (Table 3). Although most normal colon mucosa (7/10) showed only sparse methylation (Figure 5), densely methylated clones were seen in three of the ten normal colon mucosa tested (N1, N18 and N29; Figure 5). Bisulfite genomic cloning and direct sequencing also showed that methylation involving both CpG sites within the proximal and the distal region of the 5′ UTR CpG island of the *p14*^{ARF} flanking exon 1β (nucleotide position −69 to position +4 relative to the translation codon ATG) is not a frequent event in CRC, but seems to occur more particularly in tumors displaying a restricted pattern of p53 overexpression, including MSI-H and MSS tumors (Figure 5). Overall, the 3′ region of exon 1β was more densely methylated (median 41%; 95% CI 38 to 43%; range 27 to 47%) than the

Table 1 Clinicopathological and molecular data for patients analyzed by bisulfite genomic sequencing

Patient's number	Location	Type of differentiation	Stage	MMR IHC	MSI status	p53 IHC	*TP53* mutation
1	Sigmoid	Moderate	IV	Positive	MSS	D	p.R248W
3	Sigmoid	Moderate	IIIB	Positive	MSS	D	No
11	Left	Moderate	IV	Positive1	MSI-H	D	No
12	Rectum	Moderate	IIA	Positive	MSS	D	p.R273C
15	Sigmoid	Well	IV	Positive	MSS	D	p.R248Q
24	Left	Moderate	IIA	Positive	MSS	D	No
26	Rectum	Well	I	Positive	MSS	D	p.R248W
28	Rectum	Moderate	IV	Positive	MSS	D	No
30	Sigmoid	Poor	IIIB	Positive	MSS	D	p.C135R
33	Rectum	Well	IIA	Positive	MSS	D	No
34	Left	Well	IIB	Positive	MSS	D	No
35	Right	Well	IIA	Positive	MSS	D	p.[R158H (+)R267Q]
17	Sigmoid	Well	I	Positive	MSS	D	p.R248Q
2	Right	Well	IIA	MLH1-/PMS2-†	MSI-H	R	No
4	Right	Mucinous	IIIC	MLH1-/PMS2-‡	MSI-H	R	No
5	Left	Mucinous	IIA	MLH1-/PMS2-‡	MSI-H	R	No
6	Right	Well	IIA	MSH2-/MSH6-†	MSI-H	R	No
7	Right	Poor	IIA	MLH-/PMS2-‡	MSI-H	R	No
8	Left	Poor	IV	Positive	MSS	R	No
9	Right	Mucinous	IIIB	Positive	MSS	R	No
10	Right	Mucinous	IIIB	MLH1-/PMS2-†	MSI-H	R	No
13	Left	Well	IIA	Positive	MSS	R	No
14	Left	Well	IV	Positive	MSS	R	No
16	Sigmoid	Mucinous	IIA	Positive	MSS	R	No
18	Rectum	Poor	IIIC	MLH1-/PMS2-‡	MSI-H	R	No
19	Left	Well	I	MLH1-/PMS2-†	MSI-H	R	No
22	Right	Mucinous	IIIB	MLH1-/PMS2-‡	MSI-H	R	No
23	Right	Poor	IIA	MLH1-/PMS2-1	MSI-H	R	No
25	Left	Mucinous	IIA	Positive	MSS	R	No
29	Left	Moderate	IIA	Positive	MSS	R	No
20	Rectum	Moderate	IIA	Positive	MSS	N	No
21	Rectum	Mucinous	IIB	Positive	MSS	N	p.[K291X(+) H297Y]
27	Rectum	Moderate	IIA	Positive	MSS	N	c.672 + 1 G→A
31	Right	Moderate	IIIC	Positive	MSS	N	p.Q165X
32	Rectum	Moderate	IIIC	Positive	MSS	N	No

Abbreviations: MMR, DNA mismatch repair system; MSI, microsatellite instability; MSI-H, microsatellite instability-high; MSS, microsatellite-stable; IHC, immunohistochemistry; D, diffuse pattern of p53 expression, R, restricted pattern of p53 expression, N, negative pattern of p53 expression.
*MMR deficiency with unknown origin.
†Lynch syndrome.
‡Sporadic MSI-H colorectal cancer with activating V600E *BRAF* somatic mutation, indicating *MLH1* epigenetic silencing.

promoter and 5′ region of exon 1β (median 22%; 95% CI 17 to 25%; range 13 to 25%) ($P = 0.0001$) (Table 3). However, the number of methylated clones on CpG sites within the proximal region of the 5′ CpG island of $p14^{ARF}$ was significantly higher in tumors displaying a restricted pattern of p53 overexpression (median 30%; 95% CI 24 to 36%; range 17 to 36%) than in tumors exhibiting a strong diffuse p53 expression pattern (median 0%; 95% CI 0 to 3%; range 0 to 3%) ($P = 0.0003$) (Table 3).

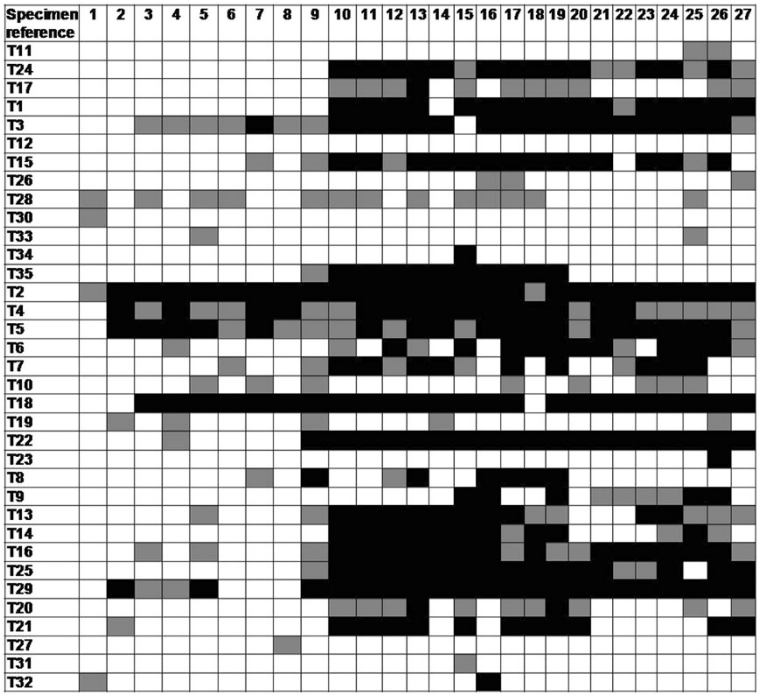

Figure 2 Heterogeneity of *p14*^{ARF} promoter methylation in colorectal tumors. The samples analyzed are represented on the horizontal line, and the 27 CpG sites on the vertical line. For each case, the methylation status of each individual CpG site is shown: an empty block indicates that the concerned CpG site is unmethylated, a black block indicates that the concerned CpG sites is fully methylated, and a gray block indicates that the concerned CpG site is partially methylated.

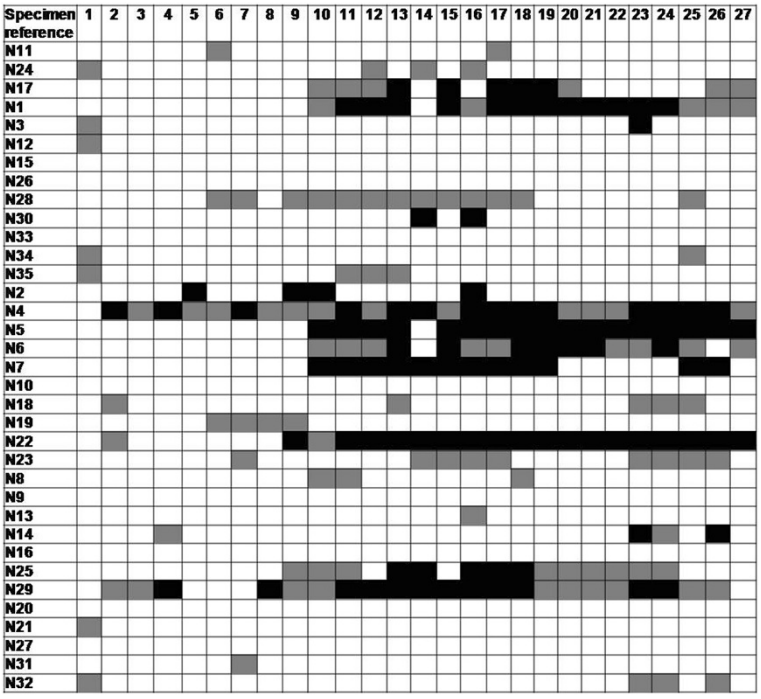

Figure 3 *p14*^{ARF} promoter methylation in adjacent colon mucosa.

Table 2 Relationships between *p14*^{ARF} promoter methylation and clinicopathological data, p53 and MDM2 protein expression, *TP53* mutational status, and microsatellite instability phenotype

Clinicopathological and molecular parameters	Overall (%)	*p14*ARF promoter methylation profile		
		Unmethylated	Dense or partial methylation	*P* value
Age, years, mean ± SD		64 ± 12	69 ± 10	0.2057[1]
Gender				
Male	16 (46%)	5 (45.5%)	11 (45.8%)	0.9833
Female	19 (54%)	6 (54.5%)	13 (54.2%)	
Type of tissue				
Tumor	35	11 (31%)	24 (69%)	0.0019
Adjacent colon mucosa	35	24 (69%)	11 (31%)	
Tumor location				
Right side	10 (29%)	3 (27.3%)	7 (29.2%)	>0.05
Left side	25 (71%)	8 (72.7%)	17 (70.8%)	
Differentiation				
Well or moderate	22 (62.9%)	10 (90.9%)	12 (50%)	0.0270
Poor or mucinous	13 (37.1%)	1 (9.1%)	12 (50%)	
Clinical stage				
Stage I	3 (8.6%)	-	3 (12.5%)	0.4674[2]
Stage II	17 (48.6%)	5 (45.4%)	12 (50%)	
Stage III	9 (25.7%)	3 (27.3%)	6 (25%)	
Stage IV	6 (17.1%)	3 (27.3%)	3 (12.5%)	
p53 immunohistochemistry				
Negative pattern	5 (14.3%)	3 (27.3%)	2 (8.3%)	0.0275[2]
Diffuse pattern	13 (37.1%)	6 (54.5%)	7 (29.2%)	
Restricted overexpression	17 (48.6%)	2 (18.2%)	15 (62.5%)	
MDM2 immunohistochemistry				
Negative	12 (34.3%)	7 (63.6%)	5 (20.8%)	0.0223
Overexpression	23 (65.7%)	4 (36.4%)	19 (79.2%)	
p21 immunohistochemistry				
Loss to mild	9 (25.7%)	6 (54.5)	3 (12.5%)	0.0146[2]
Moderate to high	26 (74.3%)	5 (45.5)	21 (87.5%)	
TP53 mutational status				
Mutation present	10 (28.6%)	5 (45.5%)	5 (20.8%)	0.2266
No mutation detected	25 (71.4%)	6 (54.5%)	19 (79.2%)	
MSI status				
MSI-H	11 (31.4%)	1 (9.1%)	10 (41.7%)	0.0539
MSS	24 (68.6%)	10 (90.9%)	14 (58.3%)	

Abbreviations: MSI, Microsatellite instability, MSI-H, microsatellite instability-high; MSS, microsatellite-stable.
[2]Two-sided two-sample *t*-test.
[2]Two-tailed Fisher's exact test.

Discussion

The purpose of this study was to investigate whether alteration of *p14*^{ARF}, a key regulator of p53-MDM2 interaction, plays a role in deregulating the p53 pathway in a subgroup of CRCs exhibiting a restricted pattern of p53 overexpression significantly associated with MSI-H phenotype, low *TP53* mutation, and MDM2 overexpression, and inversely correlated with p21 expression loss [7].

Contrary to the usual situation in solid tumor types such as melanoma, pancreatic tumors and some lung tumors [10-12], the present study confirmed the extremely low frequency of intragenic mutations and allelic losses at the *p14*^{ARF} locus in CRC [13]. Indeed, direct

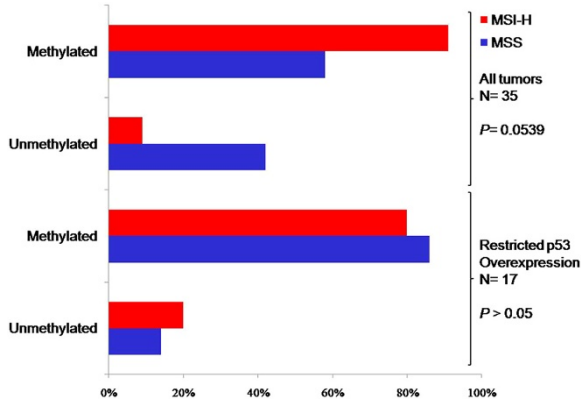

Figure 4 Relationship between *p14*^{ARF} promoter methylation and microsatellite instability (MSI) status. The MSI-high (MSI-H) tumors had an overall higher frequency of *p14*^{ARF} promoter methylation compared with MSS tumors, but after stratification by restricted p53 overexpression, the relationship between *p14*^{ARF} methylation and MSI status was no longer significant.

sequencing detected only one (previously reported) missense mutation affecting both the *p14*^{ARF} and *p16*/*CDKN2A* genes [14]. Only 5% percent of the cases, including two patients with Lynch syndrome, were carriers of p.Ala148Thr, a variant considered a non-synonymous single nucleotide polymorphisms (nsSNP, rs3731249) [14,15]. Although the functional significance of this SNP has been controversial in studies of several cancer types [15-17], its role in CRC risk assessment warrants investigation because this variant occurred at an evolutionarily conserved amino acid with a low intolerance index, as predicted by the Sorting Intolerance from Tolerance (SIFT) program [18].

We evaluated epigenetic changes within the *p14*^{ARF} promoter using two different methylation assays, MSP and BGS. We used MSP because it is widely recognized as a highly sensitive methylation assay, allowing detection of up to 0.01% of methylated alleles of a given CpG island [19]. However, this method provides only qualitative data, so for quantitative analysis, BGS complemented by cloning and direct sequencing, was used [20-22].

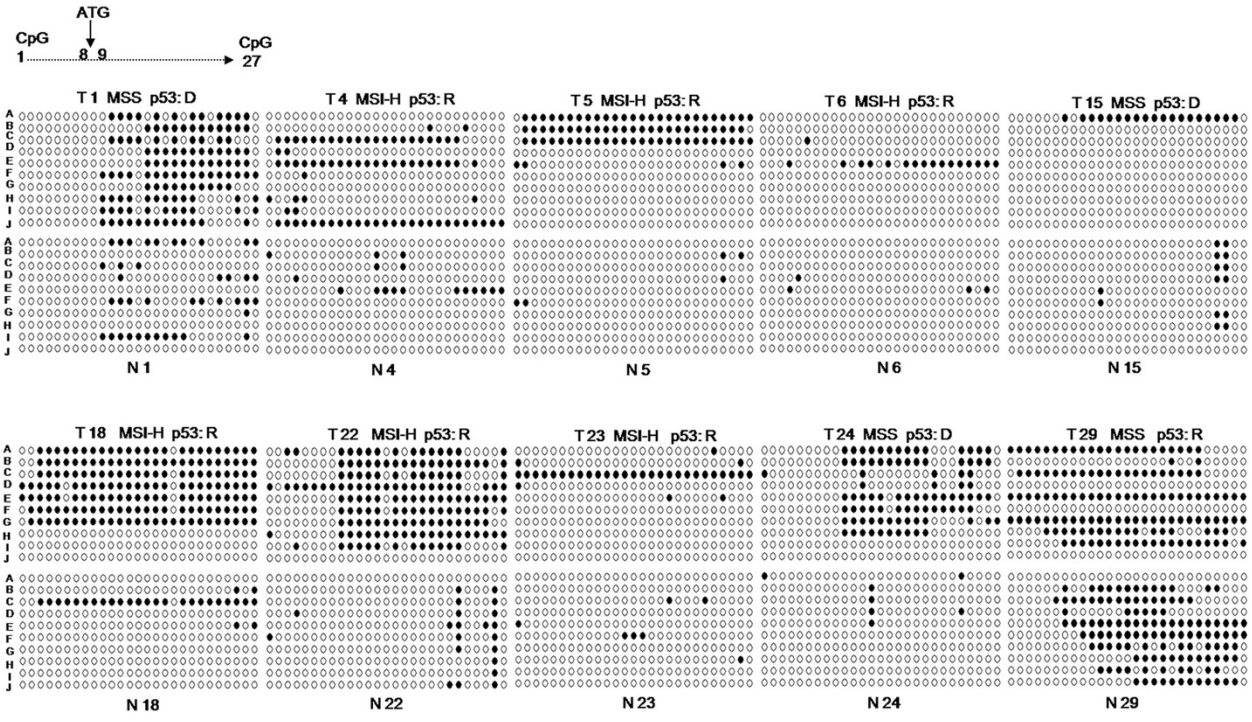

Figure 5 Density and distribution of methylated CpG within the 5′ CpG island of *p14*^{ARF} flanking exon 1β. Depicted is the distribution of methylated CpG in tumors (up) and corresponding adjacent colon mucosa (down) from 10 patients. For each case, 10 independent clones (represented on horizontal line (a) to (j) were examined. The circles on the vertical line represent the 27 CpG (CpG 1 to 27) sites analyzed for each individual clone. Note that the translation start site is located between CpG sites 8 and 9. An empty circle indicates that the concerned CpG site is unmethylated, a black circle indicates that the concerned CpG site is methylated. For each tumor, the microsatellite instability (MSI) status and p53 immunohistochemistry are indicated. MSI-H, microsatellite instability-high; MSS, microsatellite-stable; p53 D, diffuse pattern of p53 expression, p53 R, restricted pattern of p53 overexpression.

Table 3 Distribution and density of *p14*^{ARF} methylation in tumors and adjacent colon mucosa from patients with colorectal cancer

CpG site	Position relative to ATG	% of methylated clones within the 5′ CpG island flanking exon 1β			
		Tumor samples	Normal colon mucosa	Tumors with diffuse p53 overexpression pattern	Tumors with restricted p53 overexpression pattern
1	−69	13	5	3	17
2	−43	17	1	0	24
3	−40	22	1	0	31
4	−35	25	4	0	36
5	−28	22	2	0	31
6	−22	19	2	0	27
7	−10	22	5	3	30
8	−7	21	3	0	30
9	+4	30	5	3	41
10	+25	41	8	37	43
11	+31	42	12	43	41
12	+34	45	12	50	43
13	+36	43	18	43	43
14	+38	34	12	33	34
15	+42	43	13	43	43
16	+47	41	15	53	36
17	+50	45	9	50	43
18	+52	43	12	57	37
19	+66	47	9	50	46
20	+80	44	9	50	41
21	+82	40	13	37	41
22	+90	38	13	27	43
23	+105	38	13	47	34
24	+114	41	19	50	37
25	+118	34	17	37	33
26	+121	31	24	37	29
27	+133	27	9	13	33

The percentage of methylated clones was calculated in all tumors (n = 10, ≥10 clones analyzed for each tumor) and adjacent normal colon mucosa (n = 10, ≥ 10 clones analyzed for each sample) for every CpG site. The percentage of methylated clones was higher in tumors median 38%, 95% CI 25-41%; range 13-47%), than in normal colon mucosa (median 9%, 95% CI 1 to 24; range 1 to 24%) (Wilcoxon rank sum test, P <0.0001). The percentage of methylated clones on proximal CpG sites was also higher in tumors with a restricted p53 overexpression pattern (median 30%, 95% CI 24 to 36%, range 17 to 36%) than in tumors with a diffuse p53 overexpression pattern (median 0%, 95% CI 0 to 3%, range 0 to 3%) (Wilcoxon rank sum test, P = 0.0003).

Although BGS is a high-resolution assay, this technique is less sensitive than MSP as detection requires at least 25% of the alleles to be methylated [22], suggesting a risk of disagreement between the two methods.

One of our main findings was the detection of *p14*^{ARF} promoter silencing as a potential cause of deregulation of the p53-MDM2-p14^{ARF} signaling axis in a specific subgroup of CRCs. Using BGS, we fully characterized 35 of the 98 CRCs analyzed. A significant increase in *p14*^{ARF} promoter methylation was evident in 24 CRCs (69%), and interestingly, 63% of the cases (15/24) were tumors exhibiting the restricted pattern of p53 overexpression (Figure 2, Table 2).

The *p14*^{ARF} promoter has been previously reported to be preferentially hypermethylated in CRCs retaining the wild-type *TP53* gene [8,13,23], and has been particularly associated with sporadic MSI-H CRCs associated with *MLH1* epigenetic silencing [8,9]. In addition to the relationship between the restricted p53 overexpression pattern and the MSI-H phenotype [7], we found that *p14*^{ARF} promoter methylation was increased in CRCs with restricted p53 overexpression, irrespective of MSI

status (Figure 4). This observation, along with our previous findings, shows that regardless of the MSI status, CRCs with the restricted p53 overexpression pattern exhibit a significant overlap in terms of their pathobiology, supporting the hypothesis of a common tumorigenic event [7]. In agreement with these observations, previous studies have shown that although CRCs have been reported to evolve either through the classic chromosomal instability pathway or through the alternative MSI pathway known to be significantly associated with the CpG island methylator phenotype, the mechanisms underlying these genomic instability pathways are not always independent [24,25], and a significant degree of overlap can therefore be expected in some tumors, regardless of the MSI status.

Even though a high frequency of $p14^{ARF}$ promoter methylation has been previously reported to occur in tumors without *TP53* mutations [8,13,23,26], an inverse correlation between *TP53* mutations and epigenetic inactivation of $p14^{ARF}$ in CRCs does not always hold true [27]. In the current study, we found that although the majority of heavily methylated tumors did not have a *TP53* mutation, $p14^{ARF}$ promoter methylation was increased in almost half of tumors (5/10) carrying *TP53* mutations (Table 2). Interestingly, the most exceptional feature of these tumors was the distribution of $p14^{ARF}$ methylation. Using bisulfite genomic cloning and direct sequencing, we found that extensive methylation involving both the proximal and the distal CpG sites within the 5′ CpG island of $p14^{ARF}$ flanking exon 1β was rare in CRC generally, but occurred more frequently in CRCs displaying a restricted pattern of p53 overexpression (Table 3). In tumors showing a strong diffuse p53 expression pattern associated with missense *TP53* mutations, the majority of the methylated clones exhibited partial methylation involving CpG sites downstream from the translation start site and extending throughout exon 1β (Figure 5, Table 3). This pattern of methylation was also seen in some normal colon mucosa (Figure 3; Figure 5 (N29)). Our results support previous observations by Zheng *et al*., who showed that partial methylation is the most common pattern of $p14^{ARF}$ methylation in primary sporadic CRCs [28].

Owing to the limited availability of an efficient antibody raised against the $p14^{ARF}$ protein, we were unable to examine $p14^{ARF}$ expression by immunohistochemistry in our tumor samples. However, previous experiments, mainly performed in CRC cell lines, have shown that extensive methylation of CpG sites within the 5′ CpG island and exon 1β of $p14^{ARF}$ is associated with transcription silencing and correlates with extremely low levels of $p14^{ARF}$ mRNA, whereas partial methylation correlates with intermediate mRNA expression [28,29]. Based on these findings, we suggest that the extensive methylation seen in CRCs with restricted p53 overexpression may represent an important functional defect in the $p14^{ARF}$ gene, but additional studies are needed to verify this hypothesis.

Additionally, a significant relationship between MDM2 overexpression and increased $p14^{ARF}$ methylation was seen (79%; $P = 0.0223$). It is known that tumors with reduced $p14^{ARF}$ activity have higher MDM2 activity, which potentially leads to p53 inactivation [30]. Moreover, using immunohistochemistry, a strong inverse relationship between MDM2 and $p14^{ARF}$ inactivation has been previously found in different tumor types, including a subtype of human lung carcinoma displaying an abnormally stabilized p53 protein [31]. Therefore, it is conceivable that the increased MDM2 expression seen in CRCs with restricted p53 overexpression may reflect cellular functional consequences of $p14^{ARF}$ epigenetic inactivation. Interestingly, a previous study found an association between $p14^{ARF}$ epigenetic silencing and an abnormal cytoplasmic localization of MDM2 in primary CRC and tumor cell lines, mainly explained as a direct consequence of $p14^{ARF}$ loss of function [32]. In the current study, we did not find any MDM2 subcellular localization in our cohort of 98 CRCs. Functional interpretation of MDM2 immunostaining data are complicated by the existence of several isoforms, of which detection depends on the antibody used, and this may explain these discrepancies.

It is widely believed that CpG islands in autosomal genes are usually unmethylated, except when associated with certain imprinted genes and with genes that undergo X-chromosome inactivation in females [33,34]. Supporting this paradigm, initial studies indicated methylation of the 5′ CpG island of the $p14^{ARF}$ promoter exclusively in tumor cells [13,27]. However, this view was challenged by detection of $p14^{ARF}$ methylation in normal colon mucosa from patients with CRC and from healthy people without clinical evidence of colon cancer [8,35,36]. In the current study, using the MSP assay, we found coexistence of unmethylated and methylated alleles in the majority of tumors and in all adjacent normal colon mucosa. A clear difference in methylation pattern between tumor and adjacent normal colon mucosa was seen only in the seven tumors (7.1%) that showed heavy methylation. The sensitivity of our MSP assay was significantly high. However, given that we used the conventional MSP assay, which provides qualitative data, we were limited by this high sensitivity, and were unable to distinguish the $p14^{ARF}$ methylation occurring in a small proportion of cells from the high-level methylation associated with epigenetic inactivation. Using the BGS approach, we found that the level of $p14^{ARF}$ methylation in normal tissues was generally below the threshold detection of the BGS assay, and was significantly

increased in tumors compared with normal colon mucosa. However, hypermethylation was still present in normal colon mucosa from some patients, and more frequently in those with DNA mismatch repair deficiency associated with *MLH1* gene inactivation. Indeed, hypermethylation of the 5′ CpG islands of the $p14^{ARF}$ and *MLH1* genes in normal-appearing mucosa surrounding colorectal neoplastic lesions has been described as a 'field cancerization' phenomenon, which may occur before genetic alterations in the early stages of carcinogenesis [37].

Conclusion

In summary, this study provides evidence that $p14^{ARF}$ promoter hypermethylation may represent an important cause of deregulation of the p53-MDM2-$p14^{ARF}$ signaling axis in a subgroup of CRCs displaying a restricted overexpression pattern of the p53 protein, associated with the wild-type *TP53* gene, concomitant MDM2 overexpression, and normal p21 expression. Although this subgroup of CRCs includes the majority of MSI-H tumors (namely Lynch syndrome-related CRCs and sporadic MSI-H CRCs), methylation involving both proximal and distal CpG sites within the 5′ CpG island flanking exon 1β of $p14^{ARF}$ preferentially occurs in these tumors independently of MSI status. Further investigations are warranted to clarify the significance of this high-level methylation on the transcriptional activity of the $p14^{ARF}$ gene. The results from this work could have clinical implications, because therapeutic delivery of small $p14^{ARF}$ peptides has been reported to mimic the growth-inhibitory effects of full-length $p14^{ARF}$ expression and to restore p53 activity in cancers in which MDM2 is overexpressed or $p14^{ARF}$ is functionally inactivated [38]. Evaluation of the clinical relevance of such promising therapeutic measures would essentially provide a new set of more efficient treatment possibilities in patients with CRC who have tumors displaying the restricted pattern of p53 overexpression.

Methods

Ethics approval

Tissues collection and analyses were approved by the institutional ethics committee of the Catholic University of Louvain (Faculty of Medicine UCL), and all participants provided written informed consent.

Patients

We examined 98 surgical resected tumors and corresponding adjacent normal colon mucosa from the cohort of patients (48 men, 50 women, mean ± SD age 64 ± 14 years) with primary CRC we reported previously [7]. For the 98 CRCs, clinicopathologic data and evaluation of the DNA mismatch repair (MMR) system (using MSI analysis, immunohistochemistry (IHC) for MMR proteins, MMR germline mutation) and somatic *BRAF* mutation, had been performed previously [7], but only data from the 35 patients extensively studied by bisulfite genomic sequencing (BGS) are shown in Table 1. Immunohistochemical analysis for p53, MDM2, and p21 proteins and mutational analysis for *TP53* were also previously performed. Three distinct patterns of p53 expression were seen, including a restricted p53 overexpression pattern clearly distinguishable from both the negative pattern and the strong diffuse pattern [7]. MDM2 immunohistochemical expression was semi-quantitatively evaluated based on the percentage of positive tumor cells. MDM2 overexpression was recorded if a positive staining was evidenced in more than 10% of tumor cells nuclei [7].

$p14^{ARF}$ mutation screening and gene dosage

Sequence-specific primers (according to GenBank accession number NM_058195) for exon 1β and exon 2 (common to both *p16*/CDKN2A and $p14^{ARF}$), including the intronic flanking regions of the $p14^{ARF}$ gene, were designed using Primer3 software (http://frodo.wi.mit.edu/cgi-bin/primer3/primer3.cgi). PCR was carried out for each sample, and PCR products were then purified, sequenced, and run on an automated laser fluorescent DNA sequencer (3130XL; AB Applied Biosystems, Foster City, CA, USA). To detect large rearrangements (allelic imbalances) throughout the $p14^{ARF}$ locus, multiplex ligation-dependent probe amplification (MLPA) was performed using (Salsa PO24B 9p21 CDKN2A/2B region kit; MRC-Holland BV, Amsterdam, the Netherlands), in accordance with the manufacturer's instructions. MLPA PCR products were separated by capillary electrophoresis using an automated laser fluorescent DNA sequencer (3130 XL; AB Applied Biosystems, Foster City, CA, USA). The relative quantities of the amplified probes in each sample were determined using Genotyper (Applied Biosystems, Foster City, CA, USA) and Excel (Microsoft Corp., Redmond, WA, USA) software (Gene Marker version 1.5; Softgenetics Inc, State College, PA, USA). The gene dosage quotient was generated using peak height rather than peak area as an indicator of DNA template amount [39,40]. For each sample, a gene dosage quotient score (peak height relative to control) was calculated and adjusted as follows: homozygous loss ≤ 0 to 0.19 ≤ hemizygous loss ≤ 0.7 to 0.75 ≤ wild-type ≤ 1 to 1.3 < duplication.

Methylation-specific PCR

Genomic DNA was extracted from frozen tumors and matched normal tissues using a standard phenol/chloroform method. Thereafter, bisulfite treatment of 300 ng of genomic DNA was performed (Applied Biosystems

methylSEQr™ Bisulfite Conversion Kit) in accordance with the manufacturer's instructions (Applied Biosystems, Foster City, CA, USA). Methylation-specific PCR (MSP) [19] was performed to examine $p14^{ARF}$ promoter methylation within a region located at least –60 base pairs relative to the translation codon, previously reported to be associated with $p14^{ARF}$ gene silencing in CRC [27]. Methylation in this region was evaluated using the primer sets previously described [27]. These primers pairs allowed assessment of the methylation status of six CpG dinucleotides specific for the 5′ CpG island of the $p14^{ARF}$ gene flanking exon 1β (see Additional file 2: Table S1). The MSP reactions were carried out in a total volume of 25 μl containing 2.5 μl of the manufacturer's 10× PCR buffer (Roche Diagnostics, Basel, Switzerland), 1.5 μl of 25 mmol/l $MgCl_2$, and 0.25 μl of 100 μmol/l dNTPs (dATPs, dTTPs, dCTPs and dGTPs), 1 μl of primer (10 pmol/μl for each), 1 to 1.25 U of DNA polymerase (FastStart; Roche Diagnostics, Basel, Switzerland), and 1 μl of bisulfite-modified genomic DNA. Normal human leukocyte DNA was methylated in vitro with a CpG methylase (M.SssI; New England BioLabs, Beverly, MA, USA) in accordance with the manufacturer's instructions, and used as the MSP methylated-allele positive control. After amplification, 5 μl of PCR products were run in an 8% non-denaturing acrylamide gel with an appropriate size marker. Amplicons were visualized by ethidium bromide staining under UV illumination.

Bisulfite genomic sequencing

BGS primers designed to recognize both methylated and unmethylated alleles were generated based on the human contig sequence (GenBank accession number L41934) using MethPrimer software (http://www.urogene.org/methprimer/index1.html) [41]. The designed BGS primers were located within the 5′ CpG island of the $p14^{ARF}$ region flanking exon 1β, and were used to amplify a DNA sequence containing 27 CpG sites, including all the CpG sites targeted by the MSP primers within this region (see Additional file 1: Figure S1). Bisulfite-converted DNA samples from tumor tissue and corresponding adjacent normal tissues from 35 patients, randomly selected from our cohort of patients (Table 1), were subjected to PCR amplification using primer pair A and B (forward and reverse, respectively), followed by a nested PCR amplification with primer pair C and D (forward and reverse; Additional file 1: Figure S1). All the primer sequences used are summarized in (Additional file 2: Table S1). After PCR amplification, the BGS products were purified (Qiaquick PCR Purification Kit; Qiagen Inc., Valencia, CA, USA), and directly sequenced in both directions using primers C and D (forward and reverse; see Additional file 1: Figure S1) with a commercial kit (Big Dye Terminator Cycle Sequencing Ready Reaction Kit, version 1.3; Perkin Elmer/Applied Biosystems, Foster City, CA, USA) in accordance with the manufacturer's instructions. Sequencing reaction products were purified on filter plates for high-throughput separation (Multiscreen™; Millipore Corp., Bedford, MA, USA) using dextran gel beads (Sephadex™ G-50 Fine Beads; GE Healthcare Bio-Sciences AB, Uppsala, Sweden) in accordance with the manufacturer's instructions. After purification, sequencing reaction products were run on an automated laser fluorescent DNA sequencer (3130XL; AB Applied Biosystems, Foster City, CA, USA). Results were analyzed using the sequencing analysis software for the sequencer (Version 1.5; AB Applied Biosystems, Foster City, CA, USA).

For all 35 patients examined, the bisulfite sequencing chromatogram was analyzed for each individual CpG site, and a specific pattern was assigned: 1) unmethylated, in which the CpG site was fully converted into thymidine, indicating that the concerned CpG site is unmethylated on both alleles (see Additional file 3: Figure S2), 2) partial, showing an overlap of both thymidine and cytosine peaks on a sequencing chromatogram, indicating the presence of both methylated and unmethylated alleles (see Additional file 3: Figure S2 A), 3) methylated, in which the CpG site was fully methylated, indicating that the concerned CpG site is extensively methylated on both alleles (see Additional file 3: Figure S2 B).

Cloning and sequencing

For 10 patients, the amplified bisulfite PCR products from tumor and corresponding normal colon tissues were purified (Qiaquick PCR Purification Kit; Qiagen) and ligated into a pTZ57R/T plasmid vector using a TA cloning and bacterial transformation system (Ins TAclone™ PCR Cloning Kit). The plasmid was inserted into Escherichia coli cells, which were cultured overnight, then recombinant plasmid DNA was isolated and purified (Rapid Miniprep Plasmid Purification System; Marligen Bioscience, Ijamsville, Maryland, USA). Purified plasmid recombinant DNA was subjected to direct PCR amplification in a 25 μl reaction mixture containing 2.5 μl of the manufacturer's 10× PCR buffer (Roche Diagnostics, Basel, Switzerland), 1.5 μl of 25 mmol/l $MgCl_2$, and 0.25 μl of 100 μmol/l dNTPs, 1 μl of M13 forward and reverse primer (10 pmol/μl for each), 1 U of DNA polymerase (FastStart; Roche Diagnostics, Basel, Switzerland), and 1 μl of purified recombinant plasmid DNA template. Direct sequencing was performed in both directions using M13 primers with a commercial kit (Big Dye Terminator Cycle Sequencing Ready Reaction Kit, version 1.3; Perkin Elmer/Applied Biosystems, Foster City, CA, USA) in accordance with the manufacturer's instructions. Sequencing reaction products were purified

on filter plates for high-throughput separations Multiscreen™; Millipore Corp., Bedford, MA01730 USA) using dextran gel beads (Sephadex™ G-50 Fine Beads; GE Healthcare Bio-Sciences AB, Uppsala, Sweden) and were run on an automated laser fluorescent DNA sequencer (3130XL; AB Applied Biosystems, Foster City, CA, USA). For each sample, at least 10 clones were analyzed. For each clone, the bisulfite genomic sequence was analyzed, and for each individual CpG site a methylation status was assigned.

Statistical analysis

We used the Pearson χ^2 test (when the minimum expected value was ≥ 5) or the two-tailed Fisher's exact test (when the minimum expected value was <5) to compare the frequency of $p14^{ARF}$ promoter methylation in 35 patients with CRC in relation to various clinicopathologic parameters and characteristics, including immunohistochemical expression of p53, MDM2, and p21, p53 mutational status and MSI status. Comparison in distribution and density of methylation between tumors and adjacent normal-appearing colon mucosa, and of tumor groups were assessed using the Mann–Whitney or Wilcoxon rank sum test. All statistical analyses were performed using the NCSS 2007 statistical & Power analysis software. All reported P-values were two sided, and the test was significant when the $P \leq 0.05$.

Additional files

Additional file 1: Figure S1 $p14^{ARF}$ promoter methylation analysis by bisulfite genomic sequencing (BGS). The genomic sequence of 5′ CpG island of $p14^{ARF}$ region flanking exon 1β was analyzed. The highlighted and numbered CpG indicates the 27 potential CpG sites analyzed. Bold arrows indicate position of forward and reverse MSP primers for methylated (MSPMF/MSPMR) and for unmethylated (MSPUF/MSPUR) alleles. Simple arrows indicate bisulfite genomic sequencing primers specific for both unmethylated and methylated sequences. The putative transcription start site, translation start site (+1), and the end of exon 1β (*) are indicated.

Additional file 2: Table S1. Primer sequences for methylation-specific PCR, bisulfite genomic sequencing, and PCR amplification of exon 1β and exon 2 of the $p14^{ARF}$ gene.

Additional file 3: Figure S2. Bisulfite DNA sequencing chromatograms representing the three different methylation profiles for single CpG dinucleotide sites. (A) DNA sequences from tumor samples showing an overlap of both thymidine and cytosine peaks indicating a partial methylation on CpG site located at position −31 relative to the translation start site (top) compared with another sample showing an unmethylated profile at the same CpG site (bottom), (B) DNA sequences from tumor samples showing full methylation on CpG sites located at +31 and +42 relative to the translation start site (top) compared with another sample showing an unmethylated profile at the same CpG sites (bottom).

Abbreviations

CRC: Colorectal cancer; IHC: Immunohistochemistry; MLPA: Multiplex ligation-dependent probe amplification; MSI: Microsatellite instability, MSI-H, Microsatellite instability-high; MSI-L: Microsatellite instability-low, MSP, Methylation-specific PCR; MSS: Microsatellite-stable; nsSNP: non-synonymous single nucleotide polymorphism; PCR: polymerase chain reaction; UV: Ultraviolet.

Competing interests

The authors have no competing interests to disclose.

Authors' contributions

CN participated in the design of the study, carried out the pathological and molecular genetic studies, and drafted the manuscript. CS participated in the design of the study and collection of pathological data, and revised the manuscript. RD and AK participated in collection of patients. KD conceived and coordinated the study, and drafted the manuscript. All authors have read and approved the final manuscript.

Acknowledgements

We are particularly grateful to the staff members of the pathology and genetics departments for their excellent technical assistance. This study was supported by a CPTCR grant (Clinique des Pathologies Tumorales du Colon et du Rectum), Université Catholique de Louvain, Cliniques universitaires Saint-Luc, Avenue Hippocrate 10, B-1200 Brussels, Belgium.

Author details

[1]Center for Human Genetics, Université Catholique de Louvain, Cliniques universitaires Saint-Luc, Avenue Hippocrate 10, Brussels B-1200, Belgium. [2]Department of Pathology, Université Catholique de Louvain, Cliniques universitaires Saint-Luc, Avenue Hippocrate 10, Brussels B-1200, Belgium. [3]Colorectal Surgery, School of Medicine, Université Catholique de Louvain, Cliniques universitaires Saint-Luc, Avenue Hippocrate 10, Brussels B-1200, Belgium. [4]Institute of Pathology and Genetics, Avenue Georges Lemaître 25, Gosselies 6041, Belgium.

Received: 19 January 2012 Accepted: 7 May 2012
Published: 15 June 2012

References

1. Oren M, Damalas A, Gottlieb T, Michael D, Taplick J, Leal JF, Maya R, Moas M, Seger R, Taya Y, Ben-Ze'ev A: **Regulation of p53: intricate loops and delicate balances.** *Biochem Pharmacol* 2002, **64:**865–871.
2. Harris SL, Levine AJ: **The p53 pathway: positive and negative feedback loops.** *Oncogene* 2005, **24:**2899–2908.
3. Lavin MF, Gueven N: **The complexity of p53 stabilization and activation.** *Death Differ* 2006, **13**:941–950.
4. Vogelstein B, Lane D, Levine AJ: **Surfing the p53 network.** *Nature* 2000, **408:**307–310.
5. Olivier M, Eeles R, Hollstein M, Khan MA, Harris CC, Hainaut P: **The IARC TP53 database: new online mutation analysis and recommendations to users.** *Hum Mutat* 2002, **19:**607–614.
6. Rodrigues NR, Rowan A, Smith ME, Kerr IB, Bodmer WF, Gannon JV, Lane DP: **p53 mutations in colorectal cancer.** *Proc Natl Acad Sci U S A* 1990, **87:**7555–7559.
7. Christine N, Anne J-M, Alex K, Philippe C, Olivier P, Roger D, Karin D, Christine S: **Distinctive patterns of p53 protein expression and microsatellite instability in human colorectal cancer.** *Human Path* 2011, **42:**1897–1910.
8. Shen L, Kondo Y, Hamilton SR, Rashid A, Issa JP: **P14 methylation in human colon cancer is associated with microsatellite instability and wild-type p53.** *Gastroenterology* 2003, **124:**626–633.
9. Lind GE, Thorstensen L, Lovig T, Meling GI, Hamelin R, Rognum TO, Esteller M, Lothe RA: **A CpG island hypermethylation profile of primary colorectal carcinomas and colon cancer cell lines.** *Mol Cancer* 2004, **3:**28.
10. Sharpless E, Chin L: **The INK4a/ARF locus and melanoma.** *Oncogene* 2003, **22:**3092–3098.
11. Sato M, Takahashi K, Nagayama K, Arai Y, Ito N, Okada M, Minna JD, Yokota J, Kohno T: **Identification of chromosome arm 9p as the most frequent target of homozygous deletions in lung cancer.** *Genes Chromosomes Cancer* 2005, **44:**405–414.
12. Goldstein AM, Chan M, Harland M, Gillanders EM, Hayward NK, Avril MF, Azizi E, Bianchi-Scarra G, Bishop DT, Bressac-de Paillerets B, Bruno W, Calista D, Cannon Albright LA, Demenais F, Elder DE, Ghiorzo P, Gruis NA, Hansson J, Hogg D, Holland EA, Kanetsky PA, Kefford RF, Landi MT, Lang J, Leachman SA, Mackie RM, Magnusson V, Mann GJ, Niendorf K, Newton Bishop J, Palmer JM, Puig S, Puig-Butille JA, de Snoo FA, Stark M, Tsao H, Tucker MA, Whitaker L, Yakobson E, Melanoma Genetics Consortium (GenoMEL): **High-risk melanoma susceptibility**

genes and pancreatic cancer, neural system tumors, and uveal melanoma across GenoMEL. *Cancer Res* 2006, **66:**9818–9828.
13. Burri N, Shaw P, Bouzourene H, Sordat I, Sordat B, Gillet M, Schorderet D, Bosman FT, Chaubert P: **Methylation silencing and mutations of the p14ARF and p16INK4a genes in colon cancer.** *Lab Invest* 2001, **81:**217–229.
14. FitzGerald MG, Harkin DP, Silva-Arrieta S, MacDonald DJ, Lucchina LC, Unsal H, O'Neill E, Koh J, Finkelstein DM, Isselbacher KJ, Sober AJ, Haber DA: **Prevalence of germ-line mutations in p16, p19ARF, and CDK4 in familial melanoma: analysis of a clinic-based population.** *Proc Natl Acad Sci U S A* 1996, **93:**8541–8545.
15. Debniak T, Gorski B, Huzarski T, Byrski T, Cybulski C, Mackiewicz A, Gozdecka-Grodecka S, Gronwald J, Kowalska E, Haus O, Grzybowska E, Stawicka M, Swiec M, Urbański K, Niepsuj S, Waśko B, Góźdź S, Wandzel P, Szczylik C, Surdyka D, Rozmiarek A, Zambrano O, Posmyk M, Narod SA, Lubinski J: **A common variant of CDKN2A (p16) predisposes to breast cancer.** *J Med Genet* 2005, **42:**763–765.
16. Hung RJ, Boffetta P, Canzian F, Moullan N, Szeszenia-Dabrowska N, Zaridze D, Lissowska J, Rudnai P, Fabianova E, Mates D, Foretova L, Janout V, Bencko V, Chabrier A, Landi S, Gemignani F, Hall J, Brennan P: **Sequence variants in cell cycle control pathway, X-ray exposure, and lung cancer risk: a multicenter case–control study in Central Europe.** *Cancer Res* 2006, **66:**8280–8286.
17. Pjanova D, Engele L, Randerson-Moor JA, Harland M, Bishop DT, Newton Bishop JA, Taylor C, Debniak T, Lubinski J, Kleina R, Heisele O: **CDKN2A and CDK4 variants in Latvian melanoma patients: analysis of a clinic-based population.** *Melanoma Res* 2007, **17:**185–191.
18. Ng PC, Henikoff S: **Predicting deleterious amino acid substitutions.** *Genome Res* 2001, **11:**863–874.
19. Herman JG, Graff JR, Myohanen S, Nelkin BD, Baylin SB: **Methylation-specific PCR: a novel PCR assay for methylation status of CpG islands.** *Proc Natl Acad Sci U S A* 1996, **93:**9821–9826.
20. Frommer M, McDonald LE, Millar DS, Collis CM, Watt F, Grigg GW, Molloy PL, Paul CL: **A genomic sequencing protocol that yields a positive display of 5-methylcytosine residues in individual DNA strands.** *Proc Natl Acad Sci U S A* 1992, **89:**1827–1831.
21. Clark SJ, Harrison J, Paul CL, Frommer M: **High sensitivity mapping of methylated cytosines.** *Nucleic Acids Res* 1994, **22:**2990–2997.
22. Myohanen S, Wahlfors J, Janne J: **Automated fluorescent genomic sequencing as applied to the methylation analysis of the human ornithine decarboxylase gene.** *DNA Seq* 1994, **5:**1–8.
23. Tachibana M, Kawamata H, Fujimori T, Omotehara F, Horiuchi H, Ohkura Y, Igarashi S, Kotake K, Kubota K: **Dysfunction of p53 pathway in human colorectal cancer: analysis of p53 gene mutation and the expression of the p53-associated factors p14ARF, p33ING1, p21WAF1 and MDM2.** *Int J Oncol* 2004, **25:**913–920.
24. Goel A, Arnold CN, Niedzwiecki D, Chang DK, Ricciardiello L, Carethers JM, Dowell JM, Wasserman L, Compton C, Mayer RJ, Bertagnolli MM, Boland CR: **Characterization of sporadic colon cancer by patterns of genomic instability.** *Cancer Res* 2003, **63:**1608–1614.
25. Ottini L, Falchetti M, Lupi R, Rizzolo P, Agnese V, Colucci G, Bazan V, Russo A: **Patterns of genomic instability in gastric cancer: clinical implications and perspectives.** *Ann Oncol* 2006, **17**(Suppl 7):vii97–vii102.
26. Amatya VJ, Takeshima Y, Inai K: **Methylation of p14(ARF) gene in meningiomas and its correlation to the p53 expression and mutation.** *Mod Pathol* 2004, **17:**705–710.
27. Esteller M, Tortola S, Toyota M, Capella G, Peinado MA, Baylin SB, Herman JG: **Hypermethylation-associated inactivation of p14(ARF) is independent of p16(INK4a) methylation and p53 mutational status.** *Cancer Res* 2000, **60:**129–133.
28. Zheng S, Chen P, McMillan A, Lafuente A, Lafuente MJ, Ballesta A, Trias M, Wiencke JK: **Correlations of partial and extensive methylation at the p14 (ARF) locus with reduced mRNA expression in colorectal cancer cell lines and clinicopathological features in primary tumors.** *Carcinogenesis* 2000, **21:**2057–2064.
29. Robertson KD, Jones PA: **The human ARF cell cycle regulatory gene promoter is a CpG island which can be silenced by DNA methylation and down-regulated by wild-type p53.** *Mol Cell Biol* 1998, **18:**6457–6473.
30. Momand J, Wu HH, Dasgupta G: **MDM2–master regulator of the p53 tumor suppressor protein.** *Gene* 2000, **242:**15–29.
31. Eymin B, Gazzeri S, Brambilla C, Brambilla E: **Mdm2 overexpression and p14(ARF) inactivation are two mutually exclusive events in primary human lung tumors.** *Oncogene* 2002, **21:**2750–2761.
32. Esteller M, Cordon-Cardo C, Corn PG, Meltzer SJ, Pohar KS, Watkins DN, Capella G, Peinado MA, Matias-Guiu X, Prat J, Baylin SB, Herman JG: **p14ARF silencing by promoter hypermethylation mediates abnormal intracellular localization of MDM2.** *Cancer Res* 2001, **61:**2816–2821.
33. Razin A, Cedar H: **DNA methylation and genomic imprinting.** *Cell* 1994, **77:**473–476.
34. Riggs AD, Pfeifer GP: **X-chromosome inactivation and cell memory.** *Trends Genet* 1992, **8:**169–174.
35. Sato F, Harpaz N, Shibata D, Xu Y, Yin J, Mori Y, Zou TT, Wang S, Desai K, Leytin A, Selaru FM, Abraham JM, Meltzer SJ: **Hypermethylation of the p14 (ARF) gene in ulcerative colitis-associated colorectal carcinogenesis.** *Cancer Res* 2002, **62:**1148–1151.
36. Ye C, Shrubsole MJ, Cai Q, Ness R, Grady WM, Smalley W, Cai H, Washington K, Zheng W: **Promoter methylation status of the MGMT, hMLH1, and CDKN2A/p16 genes in non-neoplastic mucosa of patients with and without colorectal adenomas.** *Oncol Rep* 2006, **16:**429–435.
37. Ramirez N, Bandres E, Navarro A, Pons A, Jansa S, Moreno I, Martínez-Rodenas F, Zárate R, Bitarte N, Monzó M, García-Foncillas J: **Epigenetic events in normal colonic mucosa surrounding colorectal cancer lesions.** *Eur J Cancer* 2008, **44:**2689–2695.
38. Midgley CA, Desterro JM, Saville MK, Howard S, Sparks A, Hay RT, Lane DP: **An N-terminal p14ARF peptide blocks Mdm2-dependent ubiquitination in vitro and can activate p53 in vivo.** *Oncogene* 2000, **19:**2312–2323.
39. Schouten JP, McElgunn CJ, Waaijer R, Zwijnenburg D, Diepvens F, Pals G: **Relative quantification of 40 nucleic acid sequences by multiplex ligation-dependent probe amplification.** *Nucleic Acids Res* 2002, **30:**e57.
40. Hogervorst FB, Nederlof PM, Gille JJ, McElgunn CJ, Grippeling M, Pruntel R, Regnerus R, van Welsem T, van Spaendonk R, Menko FH, Kluijt I, Dommering C, Verhoef S, Schouten JP, van't Veer LJ, Pals G: **Large genomic deletions and duplications in the BRCA1 gene identified by a novel quantitative method.** *Cancer Res* 2003, **63:**1449–1453.
41. Li LC, Dahiya R: **MethPrimer: designing primers for methylation PCRs.** *Bioinformatics* 2002, **18:**1427–1431.

doi:10.1186/1868-7083-4-9
Cite this article as: Nyiraneza *et al.*: Hypermethylation of the 5′ CpG island of the $p14^{ARF}$ flanking exon 1β in human colorectal cancer displaying a restricted pattern of p53 overexpression concomitant with increased MDM2 expression. *Clinical Epigenetics* 2012 **4**:9.